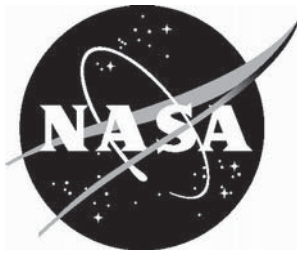


NASA/TM-2015-218701



Transient Thermal Testing and Analysis of a Thermally Insulating Structural Sandwich Panel

*Max L. Blosser, Kamran Daryabeigi, R. Keith Bird, and Jeffrey R. Knutson
Langley Research Center, Hampton, Virginia*

March 2015

NASA STI Program . . . in Profile

Since its founding, NASA has been dedicated to the advancement of aeronautics and space science. The NASA scientific and technical information (STI) program plays a key part in helping NASA maintain this important role.

The NASA STI program operates under the auspices of the Agency Chief Information Officer. It collects, organizes, provides for archiving, and disseminates NASA's STI. The NASA STI program provides access to the NTRS Registered and its public interface, the NASA Technical Reports Server, thus providing one of the largest collections of aeronautical and space science STI in the world. Results are published in both non-NASA channels and by NASA in the NASA STI Report Series, which includes the following report types:

- **TECHNICAL PUBLICATION.** Reports of completed research or a major significant phase of research that present the results of NASA Programs and include extensive data or theoretical analysis. Includes compilations of significant scientific and technical data and information deemed to be of continuing reference value. NASA counter-part of peer-reviewed formal professional papers but has less stringent limitations on manuscript length and extent of graphic presentations.
- **TECHNICAL MEMORANDUM.** Scientific and technical findings that are preliminary or of specialized interest, e.g., quick release reports, working papers, and bibliographies that contain minimal annotation. Does not contain extensive analysis.
- **CONTRACTOR REPORT.** Scientific and technical findings by NASA-sponsored contractors and grantees.

- **CONFERENCE PUBLICATION.** Collected papers from scientific and technical conferences, symposia, seminars, or other meetings sponsored or co-sponsored by NASA.
- **SPECIAL PUBLICATION.** Scientific, technical, or historical information from NASA programs, projects, and missions, often concerned with subjects having substantial public interest.
- **TECHNICAL TRANSLATION.** English-language translations of foreign scientific and technical material pertinent to NASA's mission.

Specialized services also include organizing and publishing research results, distributing specialized research announcements and feeds, providing information desk and personal search support, and enabling data exchange services.

For more information about the NASA STI program, see the following:

- Access the NASA STI program home page at <http://www.sti.nasa.gov>
- E-mail your question to help@sti.nasa.gov
- Phone the NASA STI Information Desk at 757-864-9658
- Write to:
NASA STI Information Desk
Mail Stop 148
NASA Langley Research Center
Hampton, VA 23681-2199

NASA/TM-2015-218701



Transient Thermal Testing and Analysis of a Thermally Insulating Structural Sandwich Panel

*Max L. Blosser, Kamran Daryabeigi, R. Keith Bird, and Jeffrey R. Knutson
Langley Research Center, Hampton, Virginia*

National Aeronautics and
Space Administration

Langley Research Center
Hampton, Virginia 23681-2199

March 2015

Acknowledgments

The authors would like to acknowledge Joel Alexa and Ronald Penner for their efforts in developing and implementing techniques for joining the multiple components into integrated structural panels. In addition, the authors would like to acknowledge the efforts of Vaughn Behan for developing a geometric model and detailed drawings for fabrication of panel components. Mr. Alexa, Mr. Penner, and Mr. Behan conducted their work under contract NNL07AM07T with NASA Langley Research Center. Furthermore, the authors would like to acknowledge Wayne Geouge from NASA Langley Research Center for thermal instrumentation of the panel and installation of the flexible insulation in the panel.

The use of trademarks or names of manufacturers in this report is for accurate reporting and does not constitute an official endorsement, either expressed or implied, of such products or manufacturers by the National Aeronautics and Space Administration.

Available from:

NASA STI Program / Mail Stop 148
NASA Langley Research Center
Hampton, VA 23681-2199
Fax: 757-864-6500

THIS PAGE INTENTIONALLY LEFT BLANK

Abstract

A core configuration was devised for a thermally insulating structural sandwich panel. Two titanium prototype panels were constructed to illustrate the proposed sandwich panel geometry. The core of one of the titanium panels was filled with Saffil[®] alumina fibrous insulation and the panel was tested in a series of transient thermal tests. Finite element analysis was used to predict the thermal response of the panel using one- and two-dimensional models. Excellent agreement was obtained between predicted and measured temperature histories.

Introduction

Thermal protection systems are a critical component of hypersonic and atmospheric entry vehicles that are subjected to severe aerothermal heating. The reusable ceramic tiles and blankets of the Space Shuttle Orbiter work very well as thermal insulators, but result in a fragile, high maintenance exterior surface. An intriguing potential solution to this problem is to build the thermal insulation into the exterior vehicle wall. This approach will be difficult to achieve because it requires a light weight aerospace vehicle skin to not only carry the required mechanical loads, but also to accommodate severe transient heating with the corresponding hot outer surface and large temperature gradients through the thickness. An innovative configuration (Refs. 1-2) using advanced materials (Ref. 3) will be required to balance the inherent conflict between the need to have a structurally efficient and cohesive panel, and the need to provide an efficient thermal insulator to protect the vehicle interior. NASA pursued the development of a structurally integrated sandwich panel, leading to the testing of a prototype panel. (Ref. 4)

Design of such a vehicle skin panel will require not only the capability to predict the structural response of the panel to the mechanical loads and requirements, but also the capability to predict accurately the temperatures of all components of the panel throughout the vehicle's flight. The outer surface of the panel is subjected to severe transient aerothermal heating that results in large temperature changes and temperature gradients within the panel. These large changes in temperature of various panel components will lead to significant changes in material stiffnesses and strengths, as well as thermal stresses and/or deformations resulting from thermal expansions of the various panel components. Heat transfer within the structural components of the panel occurs through solid conduction, although both the thermal conductivity and specific heat capacity of the structural materials can vary significantly over their large operational temperature range. Heat transfer through the low density insulations that fill the volume of the core is a complex combination of solid conduction, gas conduction, and radiation. Fortunately, this complex heat transfer can be approximated accurately as a diffusion problem using an effective thermal conductivity that is a strong function of both temperature and pressure (Refs. 5– 6). Because of all the complexities in the thermal response of an insulating panel, it is important to assess the accuracy of any prediction method compared to measured temperatures from relevant thermal tests.

Developing a test of a thermally insulating structural sandwich panel under transient thermal conditions representative of atmospheric entry that will produce data useful for assessing the accuracy of numerical predictions is quite a challenge. The test should incorporate as many of the important relevant aspects of the atmospheric entry that the test is attempting to simulate. Also, boundary conditions (Ref. 7) for the test specimen should be very carefully crafted so that they are representative of the desired specimen response, fully understood, and can be readily modeled with the analytical techniques being evaluated. Inevitably, simplifications in the test will be required to accomplish the testing within the available schedule and resources. The challenge is to choose a simplified, achievable testing

approach that still captures the key responses of interest and provides measured responses that can be directly and meaningfully compared with predictions.

This paper describes a candidate configuration for a thermally insulating structural sandwich panel, numerical models for predicting the transient thermal response of the panel, transient thermal tests of a titanium prototype panel, and comparisons of measured and predicted panel temperatures. Predictions are shown to closely match both the maximum temperatures and temperature histories measured during a series of tests with different heating and pressure histories in two different gases.

Thermally Insulating Structural Sandwich Panel

A structural panel that also functions as a thermal protection system could be designed as a sandwich panel. The outer surface needs to be smooth to reduce drag and to avoid enhanced aerodynamic heating. Also, it should be strong and robust to resist handling and impact damage, yet be capable of carrying significant structural load at very high temperature. The thermal expansion coefficient of the material on the outer surface should be low to reduce deformations and thermal stresses resulting from its large changes in temperature. The panel inner surface will be designed to stay below a specified temperature limit, so it must be insulated from the hot outer surface and it should have a significant heat capacity to limit its temperature rise. To be most effective as much of the heat capacity of the structure as possible should be located away from the hot surface and any unnecessary high conductivity structural penetrations into the insulating core should be avoided. An inner surface material with high thermal conductivity will tend to reduce any local hot spots from discrete structural heat shorts through the panel interior, non-uniform heating on the outer surface, or damage to the insulating core. In addition, it may enable the use of a uniform thickness panel over a region of the vehicle surface with significant variations in aerothermal heating. It is also important for the material of the inner surface to have a low coefficient of thermal expansion, although it is less critical than for the outer surface material. (Matching the thermal expansions of the outer and inner surfaces does not help because they reach their maximum temperatures at widely different times.) Structural considerations also point toward a sandwich because it is one of the most structurally efficient panel configurations for resisting in-plane compressive and shear loading without buckling. Therefore, a sandwich with a thermally insulating core makes sense from both thermal and structural considerations.

One of the biggest challenges in developing a thermally insulating structural sandwich panel is to devise a thermally insulating core that is also adequate structurally. Such a core has inherently conflicting thermal and structural requirements. It must act as a mass efficient thermal insulator in pressures from the vacuum of space to one atmosphere and temperatures from on-orbit ambient to 1000°C or higher. The insulation must fill all the interior volume of the panel to avoid radiation heat shorts from the hot outer surface to the cooler inner surface. Structurally, the core must stabilize the face sheets to prevent them from buckling under compressive or shear loading. The core must also provide an adequate structural connection between the inner and outer face sheets so that they act as a cohesive structural panel in bending. This implies that the core provide enough shear stiffness to prevent excessive out-of-plane deformations from transverse loading and to prevent premature panel buckling from in-plane compressive loading. The core must also have sufficient through-thickness strength and stiffness to avoid premature failure. The core should either be compliant enough to accommodate the mismatched thermal growth of the outer and inner face sheets or be able to match the expansions of each face sheet closely enough to avoid excessive thermal stresses.

There are at least 3 general approaches to devising a thermally insulating structural core: 1) use a rigid, homogeneous, porous material to act as both thermal insulator and a structural core, 2) use a rigid, homogeneous, porous material that is reinforced with solid structural components, and 3) use discrete, solid, structural components to carry all structural loads and fill the remaining panel interior volume with flexible, non-load-bearing thermal insulation. The first two options require development of a low density material or foam that is chemically stable at very high temperatures, is a mass-efficient thermal insulator for severe reentry conditions, and has the strength, stiffness, and strain range required to act as a structural sandwich core. It is not obvious that suitable structural insulators exist for use as a core, and if one does not exist, it would require a substantial development effort to create such a material. The third option allows a designer to choose the thermal insulator and core structural material

separately and provides a wide range of candidate geometries for the structural components of the sandwich core. Low density, non-load-bearing, fibrous insulation can be much more mass-efficient than rigid insulators and can be readily packed around somewhat complex core structural components.

A proposed core configuration, devised using the third approach previously described, is shown in Figure 1. The inner face sheet and the structural components of the core are shown, but the outer face sheet has been removed to better illustrate the core. The green component (top hat frame) shown in the figure is a continuous thin sheet of material that has been formed or molded into a corrugated shape that would form a conventional truss-core sandwich panel. However, it has large cutouts to reduce mass and to reduce heat shorts between the inner and outer face sheets. The gold and dark blue components (double and single inserts) shown in the figure are individual pieces made from a thin sheet of material that have a perimeter with formed or molded flanges and a large central cutout to reduce mass and heat shorts between face sheets. The angled sides of these reinforcing inserts are joined to the top hat frame to form stiff, buckling resistant struts that connect the inner and outer face sheets.

The other two edges of each insert are connected to the inner and outer face sheets to provide resistance to through-thickness shear loads and face sheet buckling from in plane compressive loading. The resulting struts connecting the inner and outer face sheets in the illustrated configuration are angled only in the direction perpendicular to the corrugations of the top hat frame. A further refinement of the core configuration, angling the struts between face sheets both perpendicular to and parallel to the corrugations, may be required to provide adequate core shear stiffness for both in-plane directions. The cavity between the face sheets would be filled with low density, non-load-bearing insulation. This configuration offers many geometric and material options that can be optimized to provide the best balance between thermal and structural requirements for a particular application. Of course, there are a number of other very important design considerations that must be addressed to develop a practical, workable panel, such as panel-to-panel joints, integration with the underlying structure, pressure venting strategy, and accommodation or prevention of water ingress. However, some level of confidence in the viability of a proposed acreage panel configuration should be established before spending significant time or resources trying to address these additional issues. Specific solutions to these issues will depend strongly on the acreage panel configuration.

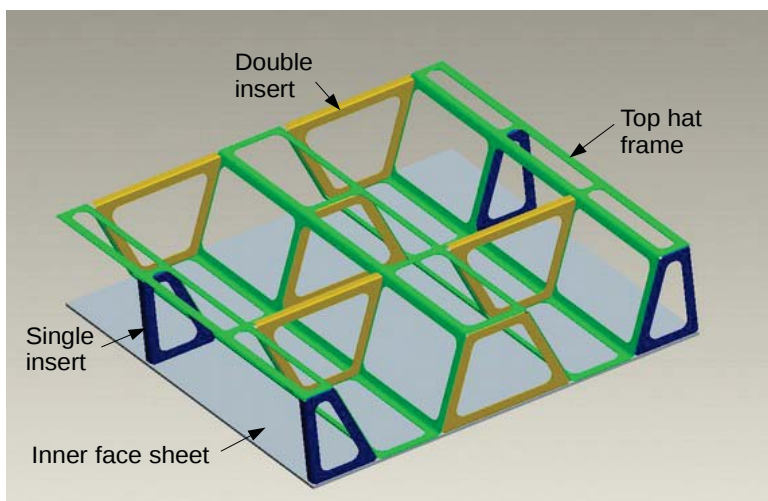


Figure 1: Proposed configuration for thermal insulating structural sandwich panel

The resulting struts connecting the inner and outer face sheets in the illustrated configuration are angled only in the direction perpendicular to the corrugations of the top hat frame. A further refinement of the core configuration, angling the struts between face sheets both perpendicular to and parallel to the corrugations, may be required to provide adequate core shear stiffness for both in-plane directions. The cavity between the face sheets would be filled with low density, non-load-bearing insulation. This configuration offers many geometric and material options that can be optimized to provide the best balance between thermal and structural requirements for a particular application. Of course, there are a number of other very important design considerations that must be addressed to develop a practical, workable panel, such as panel-to-panel joints, integration with the underlying structure, pressure venting strategy, and accommodation or prevention of water ingress. However, some level of confidence in the viability of a proposed acreage panel configuration should be established before spending significant time or resources trying to address these additional issues. Specific solutions to these issues will depend strongly on the acreage panel configuration.

Prototype Panel Fabrication

Two prototype panels, one of which is shown in Figure 2, were built from available titanium sheet material to illustrate the proposed panel geometry, as well as to get a preliminary measurement of the thermal response for this concept. Because the panel was not going to carry mechanical loads, the alloy selection was based solely on the thickness of titanium sheets on-hand in the laboratory inventory. The core components were fabricated from Ti-8Al-1Mo-



Figure 2: Titanium prototype panel

1V alloy sheet with nominal thickness of 0.025 inch. The face sheets were constructed from Ti-6Al-4V alloy sheet. The thickness of the top face sheet was 0.053 inch while the thickness of the bottom face sheet was 0.095 inch.

Each of the two square panels was 12 inches by 12 inches. The panel core consisted of one top-hat frame, four single inserts, and six double inserts. These core components were fabricated using water-jet cutting and sheet forming techniques. The components were assembled and resistance spot welded together. Small coupons were used to develop adequate spot welding parameters, but since the panels were not going to be mechanically loaded the spot welds were not optimized for strength. The top and bottom face sheets were then individually spot welded to the assembled core. The total thickness of each panel was 3.0 inches.

One of the panels was designated for thermal vacuum testing. The core framework was open enough to allow internal instrumentation (thermocouples) and fibrous insulation to be installed after the face sheets had been attached. The weight of this panel was 3.858 lbs without insulation and 4.923 lbs with insulation installed.

Transient Thermal Testing

Transient thermal tests were conducted at the NASA Langley 5-Foot Thermal Vacuum Test Facility. (Ref. 8) The overall objective of the transient thermal tests was to investigate the thermal performance of the thermally integrated structural sandwich core (TISSC) panel and validate the thermal model of TISSC. Transient thermal tests were conducted on the panel subject to various aero-heating profiles from unpublished studies of a single stage to orbit launch vehicle. This was accomplished by simultaneously varying chamber pressure and panel surface temperatures according to the generic hypersonic profiles. Maintaining one dimensional heat transfer in transient thermal testing of complex panels is not easily achievable. The test set-up used in this study was developed in order to minimize lateral heat transfer, and to result in quasi one-dimensional heat transfer in the central area of the set-up.

Test Set-up Description

A brief description of the test set-up is provided. A schematic of the overall test set-up is shown in Figure 3. The main components of the system are: quartz lamp array heater, Inconel septum plate, test panel, Min-K® guard insulation, titanium guard plate, aluminum heat sink, and the surrounding insulation which consists of BTU-BLOCK™ and refractory ceramic board insulations. (Min-K® and BTU-BLOCK™ are rigid microporous insulations manufactured by Morgan Thermal Ceramics)

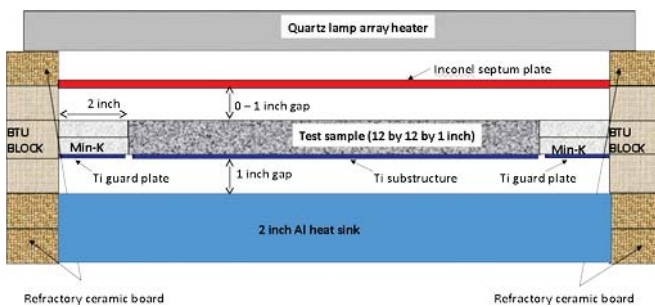


Figure 3: Schematic of transient thermal test set-up at NASA LaRC.

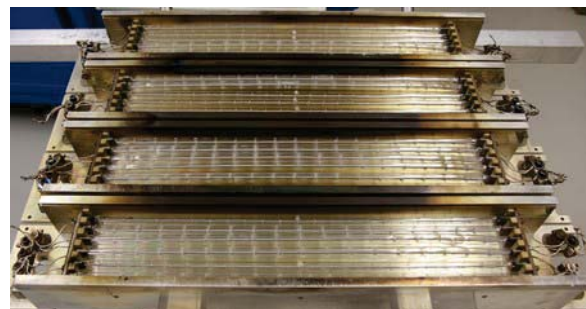


Figure 4: Quartz lamp heater

A quartz lamp array heater, shown in Figure 4, with a heated area of 16 inches by 16 inches was used as the heater for the set-up. A 16-inch by 16-inch by 0.25-inch Inconel septum plate (Figure 5) was used in between the quartz lamp heater array and the top of the test sample. The septum plate was placed one inch below the heater array, and was used to provide an approximate spatially-uniform temperature target plate boundary, which would then heat the top of the test panel. Tests were conducted with a nominal one inch gap maintained between the septum plate and the top of the test sample. Heat transfer from the septum plate to the top of the test sample was through radiation and gas

conduction modes of heat transfer. The Inconel septum plate had been previously exposed to static oxidation in an oven prior to testing in order to create stable oxide layers on both sides of the plate with an approximate effective emittance of 0.8. Four stainless steel rods, protruding from the surrounding insulation, were used to hold the septum plate in place. A photograph of the septum plate held in place in the test setup using the four stainless steel rods is shown in Figure 5.

The test set-up can be used to test panels with planar areas of 12 inches by 12 inches, while panel thickness can vary between 1 and 3 inches. The TISSC panel used in these tests had nominal dimensions of 12-inch by 12-inch by 3-inch thick. A 16-inch by 16-inch by 3-inch thick, 2-inch wide annular guard insulation was placed around the periphery of the test sample. This guard was composed of six 0.5-inch thick Min-K[®] insulation blankets with an effective density of 18 lb/ft³. Min-K[®] is a very low thermal conductivity insulation and was therefore used to minimize lateral heat losses from the peripheries of the test sample. The Min-K[®] insulation was placed on a 16-inch by 16-inch by 0.1-inch thick, 1.9-inch wide picture frame titanium guard plate, that would provide a picture frame around the inner face sheet of the test panel. A nominal 0.1-inch gap was used between the panel inner face sheet and guard titanium plate to eliminate lateral heat transfer from the edges of the test assembly to the test panel inner face sheet. Eight 1-inch by 1-inch by 1-inch SALI¹ rigid insulation board spacers were placed around the periphery of the test set-up on top of the aluminum heat sink in order to hold the titanium guard plate and the test panel in place, and maintain a one inch gap between the heat sink and bottom side of the test panel and titanium guard plate. Four of the rigid insulation board spacers were placed around the edges of the test panel, while the other four were placed around the outside edges of the titanium guard plate.

The heat sink, shown in Figure 6, consisted of two 16-inch by 16-inch by 1-inch thick aluminum plates stacked on top of each other. The bottom of the test panel and titanium guard plates and the top of the aluminum heat sink were coated with a flat black paint with an approximate total hemispherical emittance of 0.92. The back face boundary condition on the test panel consisted of radiation and gas conduction across a one-inch thick gap to an aluminum heat sink. A combination of BTU-BLOCK[™], refractory ceramic board, and Saffil[®] fibrous insulations, referred to as surrounding insulation, was used around the overall test assembly to minimize heat

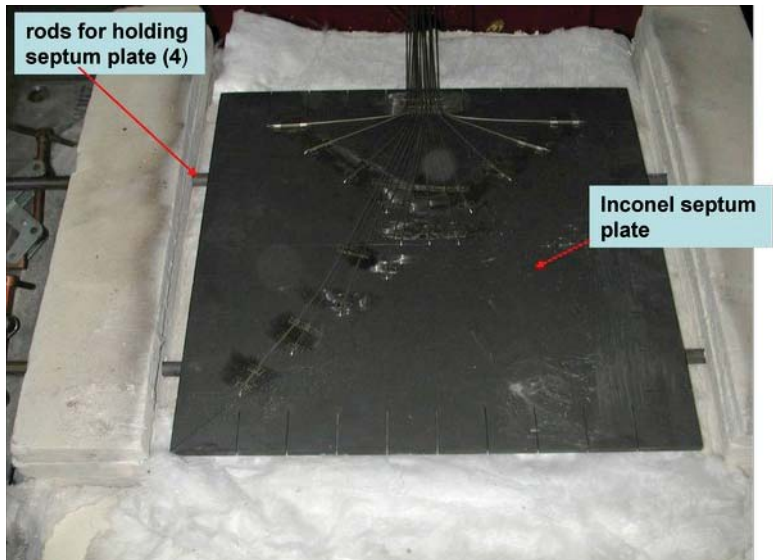


Figure 5: Inconel septum plate and four stainless steel rods for holding the septum plate

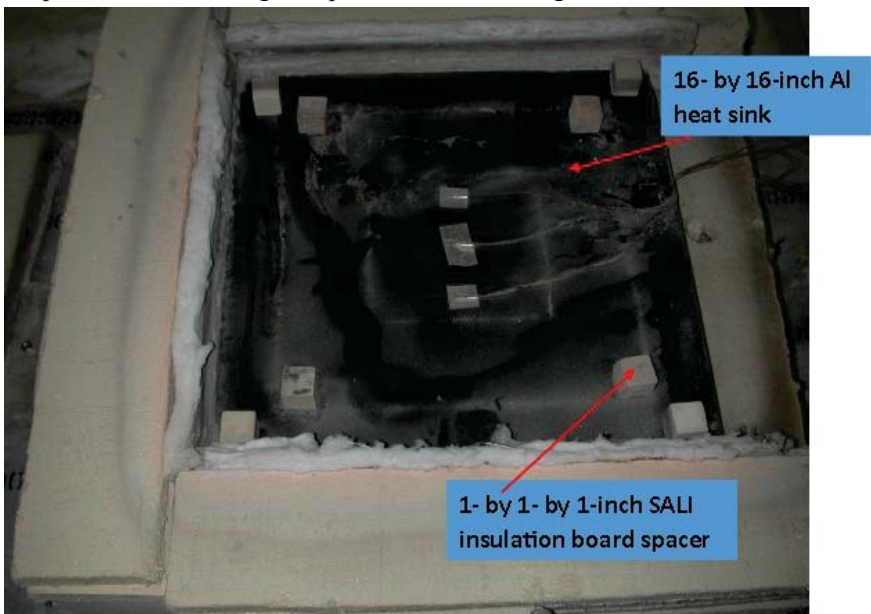


Figure 6: Aluminum heat sink and SALI insulation board spacers

¹ Zircar Ceramics

losses from the test set-up to the vacuum chamber walls. A thin layer of Saffil[®] was also utilized between the periphery of the test panel and the Min-K[®] guard insulation to prevent any direct radiation in the gap between the panel and guard insulation.

Figure 6 shows a photograph of the aluminum heat sink and the eight SALI insulation board spacers. The overall assembly was placed inside a 5-ft vacuum chamber at NASA LaRC. A photograph of the test set-up in the vacuum chamber is shown in Figure 7.

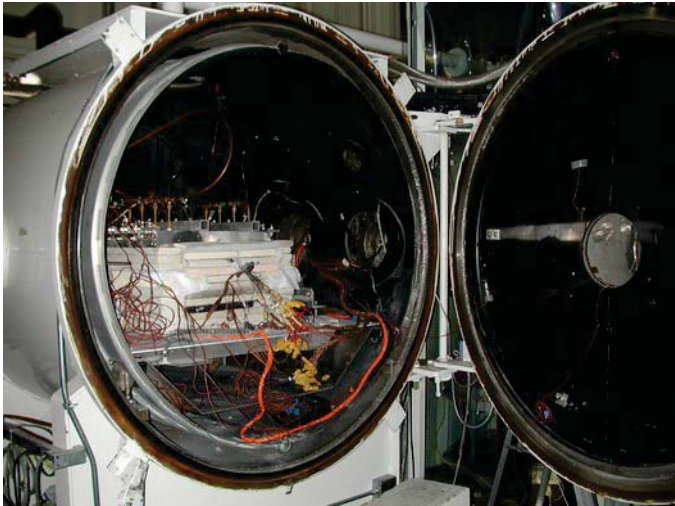


Figure 7: Test set-up in the 5-ft vacuum chamber at NASA LaRC

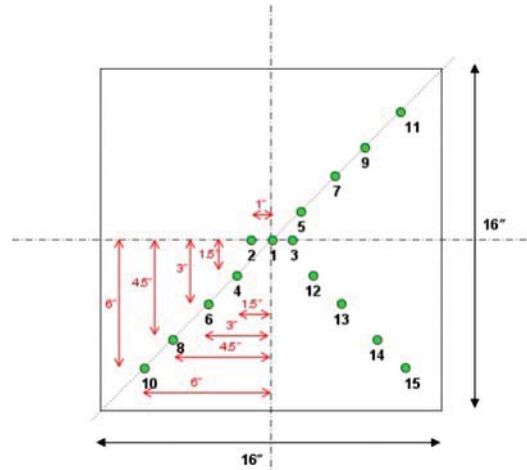


Figure 8: Thermocouple layout on the Inconel septum plate

Instrumentation

The Inconel septum plate was instrumented with 15 metal-sheathed Type K thermocouples. A schematic drawing showing the thermocouple locations is shown in Figure 8. There was redundancy in the number of thermocouples used, in case of thermocouple failure during the tests. Only six of these thermocouples were connected to the data acquisition system. One of the thermocouples was used as the control thermocouple in conjunction with a proportional, integral, derivative-based (PID) controller to control the heating from the quartz lamp array heater to achieve the desired generic transient temperature profile.

Three Type K thermocouples with fiberglass insulation were installed on the titanium guard plate. The thermocouples were installed on the backside of the titanium plates, the side facing the aluminum heat sink. These thermocouples were used to estimate the magnitude of lateral heat losses at the inner face sheet of the panel. Two Type K thermocouples with fiberglass insulation were installed on the top side of the aluminum heat sink to monitor its temperature. The average value of these two thermocouples was used to represent the heat sink temperature and was designated as T_{AL} .

The TISSC test panel was instrumented with 27 type K thermocouples. Three thermocouples were located on the outside surface of the panel outer face sheet facing the septum plate, with locations indicated by red dots on Figure 9. Four thermocouples were located on the inside surface of the panel outer face sheet, with locations indicated by green dots on Figure 9. Ten thermocouples were located on the interior of the panel at various locations on the struts, for monitoring temperatures along the titanium truss core structure, with locations indicated by the green dots in Figure 10. Four thermocouples were located on the interior surface of the panel inner face sheet, with locations indicated by green dots on Figure 11. Three additional thermocouples were placed on the exterior of the inner face sheet, with locations indicated by the blue dots on Figure 11.

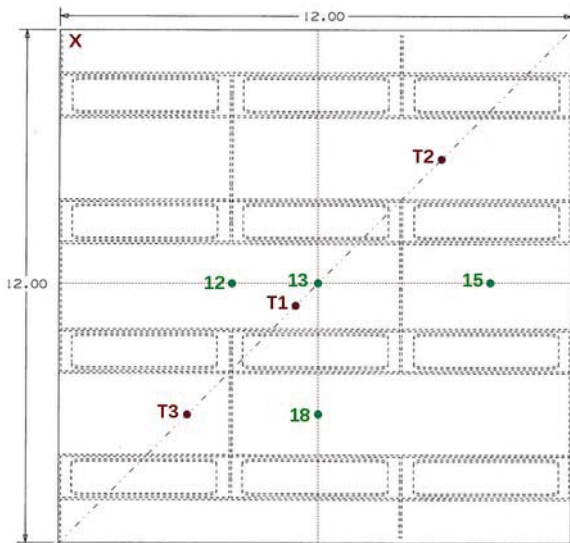


Figure 9: Thermocouple layout on the TISSC panel outer face sheet

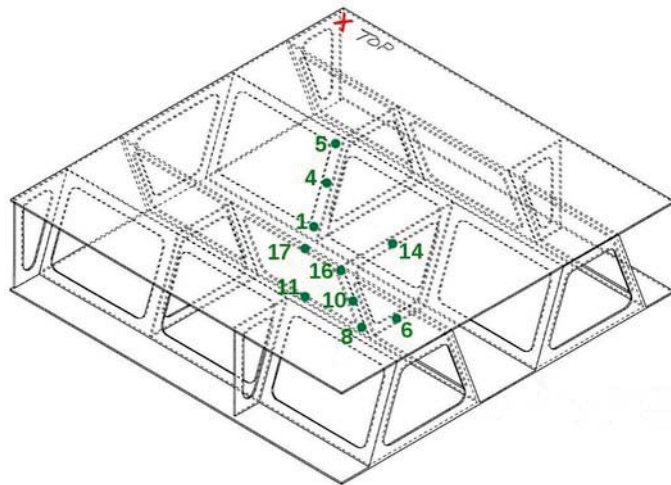


Figure 10: Thermocouple layout on the TISSC panel struts

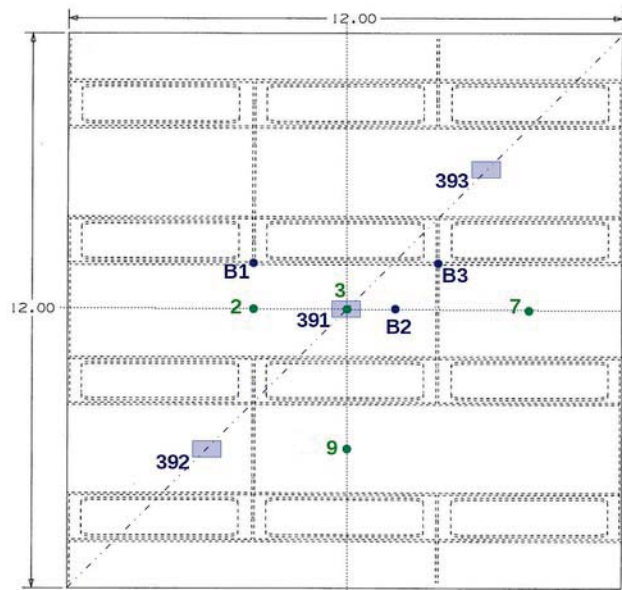


Figure 11: Instrumentation layout on the TISSC panel inner face sheet

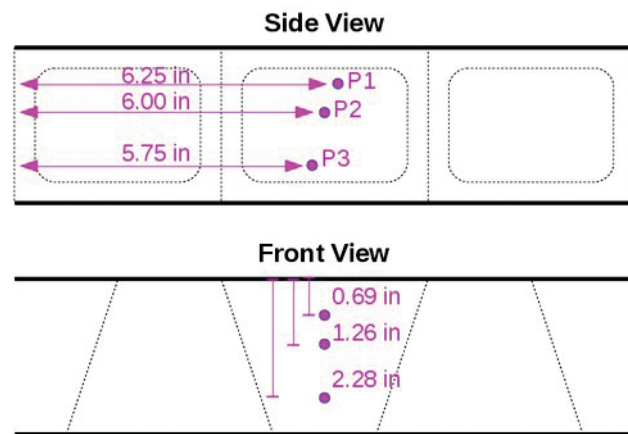


Figure 12: Insulation thermocouple locations

Three thin-film heat flux gages were also installed on the outside surface of the panel inner face sheet providing both heat flux and surface temperature data, with locations indicated by the blue rectangles on Figure 11. Three thermocouples were located inside the Saffil[®] insulation used to fill the TISSC panel as shown in Figure 12.

The overall uncertainties in the measurement of temperatures on the titanium and Inconel plates were 3.8 and 6.5°F, respectively. The various thermocouple, heat flux, and pressure data were recorded at 1 hertz.

Test Conditions

The aeroheating data from body points labeled 1 and 3 on a generic hypersonic vehicle were used for these tests. The generic transient vehicle surface temperatures for these two body points are shown in Figure 13, while the transient static pressure variation is shown in Figure 14. The maximum surface temperature for body points 1 and 3 were 1019 and 868°C, respectively. The pressure variation for the two body points was very similar, with body point 3 pressures being slightly lower than body point 1 pressures. Typically, tests are controlled by simultaneously varying the chamber static pressure and the Inconel septum plate temperature according to the profile. The heating segments of the profile, when temperatures were increasing, were controlled using PID control of the quartz lamps based on measured temperature data from one of the thermocouples on the septum plate. There is no active cooling for this test set up, so the cooling segments of the profile were not controlled, and were achieved by natural cooling in the chamber with power to the quartz lamp array cut off. The duration of the profile was 2700 seconds, but in most cases data were taken for 3600 seconds. During the extra testing period beyond the end of the profile, the chamber pressure was maintained at the pressure value at 2700 seconds, while the septum plate temperatures experienced uncontrolled drop due to natural cooling in the chamber.

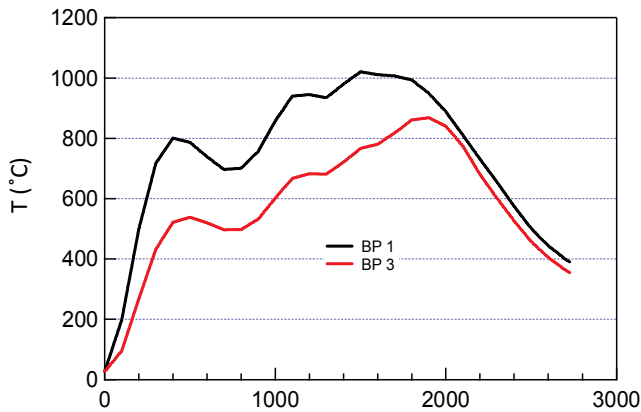


Figure 13: Transient surface temperature variations for body points 1 and 3

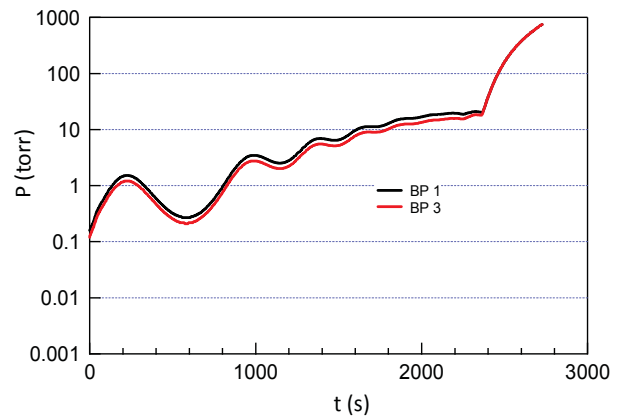


Figure 14: Transient pressure variations for body points 1 and 3

Tests were conducted in argon and nitrogen gases. Argon was originally selected as the working gas because it is inert and would not cause material changes in titanium at high temperatures. But testing in argon proved to be difficult, with electrical arcing developing between the quartz lamp array and the test panel. The electrical arcing would cause blowing of fuses, thus resulting in test termination. Therefore, the working gas for the tests was changed to nitrogen despite concerns about formation of titanium nitride at higher temperatures. A listing of all the tests is provided in Table 1. The first six tests were conducted in argon. Tests 3 and 6 experienced arcing in the chamber. Ten tests were conducted in nitrogen: tests 7 through 16.

The first 12 tests used either a constant chamber pressure of 0.001 torr, or by following the pressure profile for body point 3. For these tests, a modified temperature profile based on body point 3 temperatures was used. Because of concerns about oxidation and/or material change of titanium at higher temperatures, the temperature profiles were scaled so that the maximum test temperature was either 540, 650, or 760°C. Maximum temperatures of 540, 650, and 760°C were used for tests 1 through 4, 5 through 9, and 10 through 12, respectively. Test 13 was aborted. Tests 14 and 15 were conducted following body point 1 pressures and temperatures without any scaling of temperatures. Test 16 followed body point 1 temperatures but at a constant pressure of 1 torr.

Table 1. Listing of tests

Test No.	Working Gas	Pressure Profile	Temperature Profile	Max. Temperature for Scaling (°C)	Premature Test Termination
1	argon	Constant – 0.001 torr	Modified BP 3	540	
2	argon	BP 3	Modified BP 3	540	
3	argon	BP 3	Modified BP 3	540	Yes
4	argon	BP 3	Modified BP 3	540	
5	argon	BP 3	Modified BP 3	650	
6	argon	BP 3	Modified BP 3	650	Yes
7	nitrogen	BP 3	Modified BP 3	650	
8	nitrogen	BP 3	Modified BP 3	650	
9	nitrogen	Constant – 0.001 torr	Modified BP 3	650	
10	nitrogen	Constant – 0.001 torr	Modified BP 3	760	
11	nitrogen	BP 3	Modified BP 3	760	
12	nitrogen	BP 3	Modified BP 3	760	
13	nitrogen				Yes
14	nitrogen	BP 1	BP 1	NA	
15	nitrogen	BP 1	BP 1	NA	
16	nitrogen	Constant – 1 torr	BP 1	NA	

Transient Thermal Analysis

Modeling of Panel Flight Performance

Accurately modeling the nonlinear, transient thermal response of a thermally insulating structural sandwich panel subjected to hypersonic aerodynamic heating involves a number of challenges. A very accurate way to model the panel behavior would be to simultaneously model the entire vehicle structure and the surrounding flow field throughout a design mission. However, this approach would be quite impractical with current computers and software in terms of computational speed and capability, and would require definition of an enormous amount of detailed information that is not available or necessarily of interest to a panel analyst or designer. Even if the computational tools were available to solve the problem in very little time and all the required information was available, it would be a formidable task to correctly enter all the data into the model, make the myriad modeling decisions required, ascertain that the model is producing correct results, and sort through the large amount of calculated results to extract and understand the relevant panel responses. Therefore, there is a compelling incentive to develop a simple model that will calculate the responses of interest to an acceptable accuracy, especially if the model will be used early in the design process before vehicle and mission details have been well defined.

One of the key challenges is to define the aerothermal heating history for the surface of the panel exposed to external aerodynamic flow. Aerodynamic heating can be a combination of convective and radiative heating, but for reusable earth entry and hypersonic cruise vehicles, the heating is usually treated as entirely convective. The heating history is typically calculated for specific locations on a particular vehicle throughout a limited set of design missions using an uncoupled aerothermodynamic heating program. The aerothermodynamic heating calculation is usually decoupled from the thermal response of the vehicle surface by assuming that either the surface is adiabatic and radiating to space or by calculating the heating for a series of fixed surface temperatures that bound the expected surface temperature range. Also, any surface deformations are usually assumed to be small enough that their effect on the heating is negligible. For the adiabatic surface assumption, the heating histories are typically calculated in one of three forms: 1) radiation equilibrium surface temperature, 2) radiation equilibrium heating rate, and 3) convection coefficient with recovery temperature or enthalpy. All three options depend on an assumed surface emissivity. For the assumption of

fixed vehicle surface temperature, the heating history is given as a heating rate profile for each assumed surface temperature. The thermal analysis would then have to calculate the surface temperature and use the calculated surface temperature to interpolate between the fixed temperature profiles to find the applied heating rate.

Another challenge is to choose the extent of the panel geometry and adjacent vehicle structure to include in the model. Coupled to this choice is the selection of boundary conditions for each edge of the model not exposed to aerodynamic heating. To gain further insight into this modeling challenge, it is instructive to consider thermal analyses of reusable thermal protection systems and the underlying structure. For a detailed analysis of a well defined or existing vehicle, such as the Space Shuttle Orbiter, analysts may choose to model large sections of the vehicle structure and thermal protection system (TPS) (Refs. 9-10). However, for conceptual or preliminary design studies, a much simpler one- or two-dimensional model may be much more practical and useful (Refs. 11-13). For both the detailed and simplified models, the lateral boundaries are assumed to be adiabatic, which is the simple default boundary condition in finite element thermal analysis if nothing is specified. The adiabatic boundary condition is strictly true only if the boundary is perfectly insulated or if the boundary is on a symmetry plane for both geometry and loading. However, it is often used to simplify the model if the heat transfer through the boundary is assumed to have a minor effect on the overall performance. Using symmetry planes to model a plug from the interior of a panel would, of course, neglect lateral conduction to underlying structural reinforcements or heat transfer through panel-to-panel joints.

For the inner surface of the panel that faces the vehicle interior there are two basic options: 1) consider it adiabatic, or 2) model some mode of heat loss. The adiabatic option simplifies modeling in some ways and was used in the design of the Space Shuttle when sizing the TPS mounted on the aluminum structure of the orbiter. However, if there is no heat loss out of the inner surface and sides of the model, then the only way for heat to be removed from the inner face sheet is for it to be conducted back through the sandwich core. That means that the core must cool to below the inner face sheet temperature before the inner face sheet can reach its maximum temperature. Therefore, an adiabatic inner surface will require assuming some heat loss mechanism for the outer surface after landing and continuing the simulation for considerable additional time to capture the maximum inner surface temperature.

Modeling of Prototype Panel During Transient Thermal Test

In addition to the modeling challenges previously discussed, there are a number of test-specific considerations that must be addressed. Chiefly these challenges involve simulating the experimental boundary conditions and defining simplifying assumptions to reduce the complexity of the specimen model.

As described previously, the surface of the panel was heated using a quartz lamp heater with a septum plate between the heater and panel surface. Predicting the flux distribution from a quartz heater is complex and difficult (Ref. 14), so the septum plate is used to make the surface heat flux more uniform and easier to model. One approach is to specify the measured temperature history of the septum plate and model the heat transfer across the gap to the surface of the panel. A simpler approach, using the average measured surface temperature history of the panel as the surface boundary condition, was used for this analysis.

On the inner surface of the panel the heat transfer was modeled across the gap to the adiabatic aluminum heat sink. Both radiation and gas conduction were modeled. The well insulated perimeter of the panel was treated as adiabatic.

Rather than modeling the complex 3-dimensional geometry of the panel, simplifications were used to generate 1- and 2-dimensional models, as shown in Figure 15. Although the geometry was greatly simplified, the cross-sectional areas of all flanges and struts were carefully calculated and corrected for any angle from vertical, so that the cross-sectional areas used in the models captured the correct conductances of the metal components. The remainder of the cross-sectional area was assumed to be insulation. The sides of the models and the inner surface of the aluminum heat sink were assumed to be adiabatic. The average measured surface temperature history was imposed on the outer surface of the panel. Both gas conduction and radiation across the air gap between the panel and the heat sink were modeled. Radiation was modeled using an effective conductance calculated for the radiant exchange between two infinite gray surfaces. Both surfaces were painted with a high emissivity coating with an emissivity of 0.92.

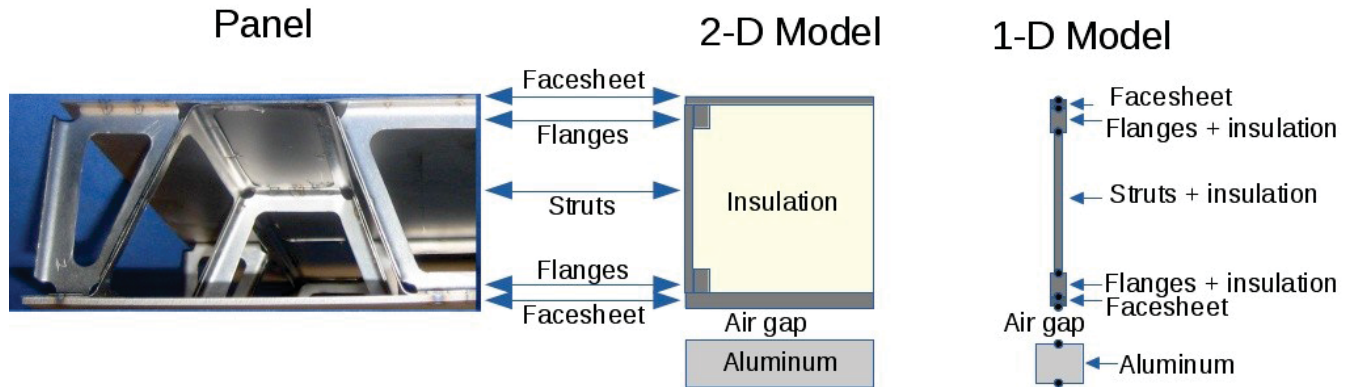


Figure 15: Modeling simplifications

The one- and two-dimensional finite element models were developed using the DOLFIN (Ref. 15) finite element library for the Python programming language. Using the DOLFIN library, linear one- or two-dimensional elements were used to discretize the spatial dimension and an implicit Crank-Nicolson time marching scheme was used to solve the weak formulation of the diffusion equation. The models are shown schematically in Figure 15. For these simplified geometries, the meshes were developed parametrically so the mesh of any component of the model could be easily changed. Although a careful convergence study was not performed, meshes were adjusted until further refinement produced temperature changes less than 0.1°C. The boundary condition on the outer surface of the panel consisted of an imposed surface temperature that could be varied arbitrarily with time and updated at each time step of the solution. The inner surface of the aluminum heat sink was adiabatic. The material properties could be arbitrary functions of temperature and ambient pressure. Material property values for each finite element were updated at each time step of the analysis for the average temperature of each element from the previous time step. Property values could be different for each element, but did not vary spatially within an element. A time step of 5 seconds was used to calculate the results presented in this paper. Accurate material properties were essential for predicting panel performance. Insulation properties as a function of temperature and pressure were calculated using methods from Ref. 5, but the properties for the Ti-8-1-1 core were measured by Thermophysical Properties Research Laboratory, Inc. (Table 2). Properties for the Ti-6-4 face sheets were from the Aerospace Metals Handbook.

Table 2: Properties for Ti-8-1-1

T, K	k, W/m ² *K	c _p , J/Kg*K
296	6.145	507
373	7.182	552
473	8.541	591
573	10.043	634
673	11.365	655
773	12.669	680
873	14.078	699
973	15.787	729
1073	17.456	760
1173	19.037	780
1273	20.999	800

Results

The experimental results were examined to determine the uniformity of heating, symmetry of the thermal response, repeatability, effect of argon vs nitrogen, effect of constant pressure vs variable pressure, and the effect of maximum applied surface temperature on the thermal response of the panel. The measured temperatures on the outer face sheet were examined to determine which experimental temperature history should be used as the applied surface temperature for the analytical models. The measured temperatures through the depth of the panel and on the inner surface were compared to temperatures predicted by the finite element models.

Uniformity of Applied Heating

Although the temperatures on the septum plate were not used directly in the finite element models, they do give some indication of the uniformity and repeatability of heating. Only the readings of the lower left quadrant of the septum plate were recorded. (TC numbers in Figure 8 are referred to as S1, S2, etc.) Although the amplitudes of the septum plate temperatures varied for the tests listed in Table 1, the temperature distributions were very similar for all tests. Typical septum plate temperature histories are shown in Figure 16 for Test 8. All of the thermocouples except S8 read nearly the same values. S8 could be reading low or it could be located directly below the small space between two of the four water cooled reflectors that make up the quartz lamp array (see Figure 4). These temperature histories indicate that most of the septum plate is nearly uniform in temperature and therefore should impose a nearly uniform heat flux on the outer face sheet of the test panel.

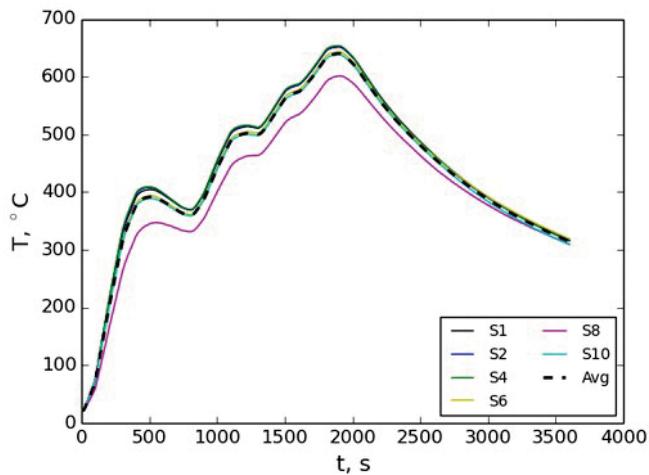


Figure 16: Septum plate temperatures for Test 8

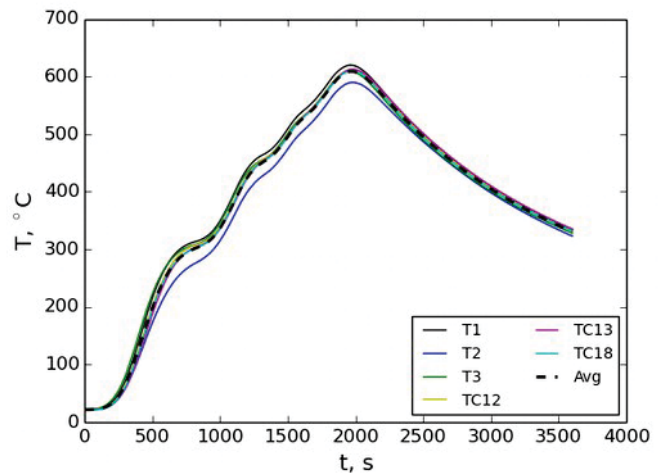


Figure 17: Outer surface temperatures for Test 8

The temperatures of the heated or outer surface of the panel were examined and found to have very similar spatial variations for all of the tests. The temperature histories for the 6 thermocouples on the outer surface of the panel during Test 8, typical of the distributions for all of the tests, are shown in Figure 17. The locations of the outer surface thermocouples are shown in Figure 9. The temperatures for five of the six thermocouples agree closely for all of the tests. However, the temperatures for T2 are consistently lower than the others for all tests. This lower temperature may indicate a problem with the thermocouple, or it may be measuring a non-uniformity in heating that results from using 4 discrete water-cooled lamp holders for the heater array – as previously described for the septum plate. The average of the six thermocouples is indicated by the dashed line in Figure 17.

The average temperatures for the hot outer surface are shown for all of the tests in Figure 18. The numbers in the legend refer to the test numbers listed in Table 1. Tests with the same nominal applied heating are depicted with the same color

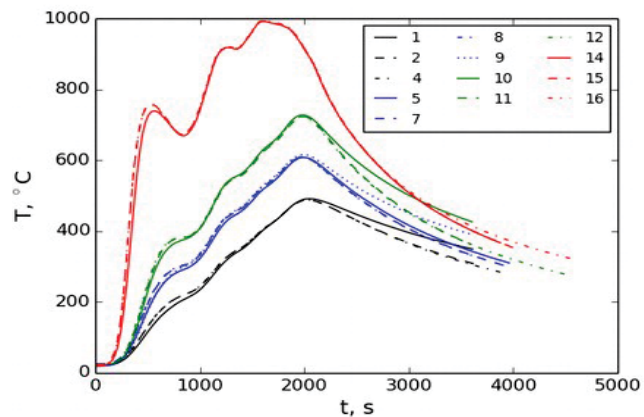


Figure 18: Average outer surface temperatures

lines, but different line patterns. The heating portion of the simulated heating histories demonstrated good repeatability. The cooling portion of the tests with variable pressure also showed good repeatability. However, for the tests with a fixed low pressure, the panel surface cooled more slowly. The average hot outer surface temperatures shown in Figure 18 were used as the imposed surface boundary temperature histories for the finite element models.

Thermal Response of Test Panel

The results for Test 8 were typical of most of the tests (Tests 2, 4, 5, 7, 8, 11, and 12). These tests were performed with three different heating histories and two different ambient gases, but all used the BP 3 pressure history shown in Figure 14. Although the amplitudes of the temperature histories varied between these tests, the trends and the comparisons between measured and predicted temperature histories were similar for each test. Temperatures were measured through the interior of the panel using thermocouples attached to the titanium struts shown in Figure 10, and embedded in the fibrous insulation as shown in Figure 12.

For Test 8, the temperatures measured on the titanium struts are shown in Figure 19. The solid lines represent the temperatures measured on one strut and the dashed lines represent temperatures measured at the same locations on an identical strut. The red lines are for temperatures near the heated surface, the magenta lines near the panel center and the green lines on the inner, unheated panel surface. The lines with a dash dot pattern represent predicted temperatures from the two-dimensional model and the dotted lines represent predicted temperatures from the one-dimensional model. There is some variation in the temperatures of the two struts, which could be caused by slight differences in thermocouple location, variation in surface heating, or variations in the panel construction (spot weld locations, etc.). Predictions from both the one- and two-dimensional models closely predict the measured response. For the location nearest the hot surface, both models slightly over predict the

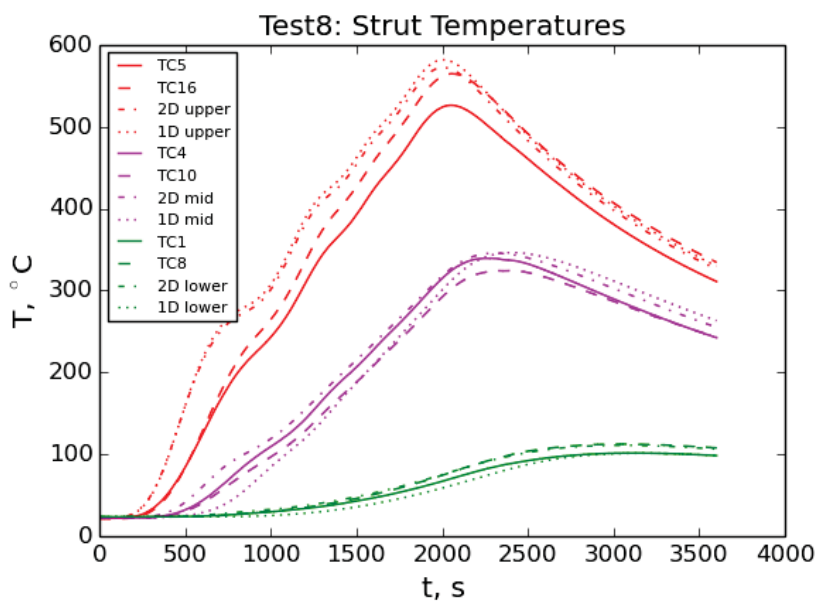


Figure 19: Temperatures of titanium strut for Test 8

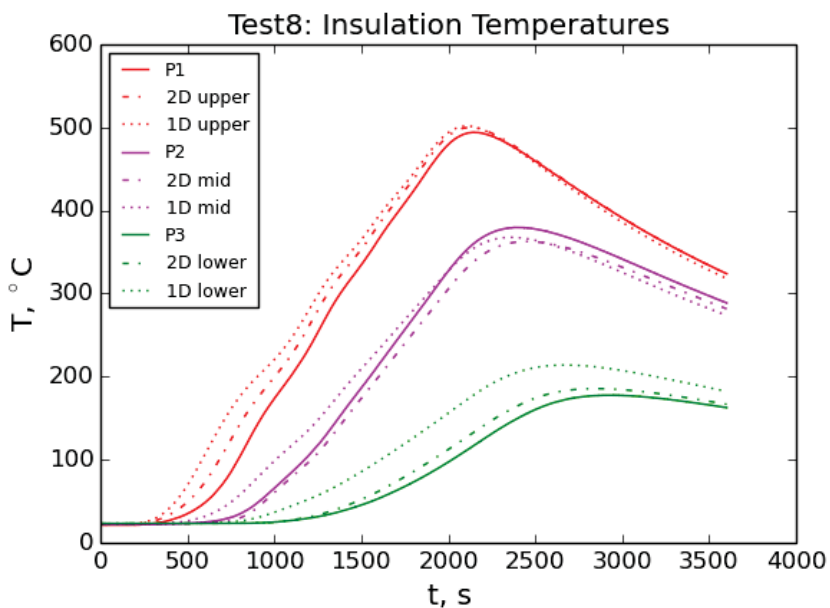


Figure 20: Temperatures for insulation in Test 8

measured temperatures. For the other two locations, the 1-D model slightly lags the 2-D model and the measured temperatures, but both models closely predict the measured temperature histories.

The temperatures measured through the depth of the insulation for Test 8 are shown in Figure 20. The solid lines represent the temperatures measured through the depth of the insulation near the center of the panel (See Figure 12 for thermocouple locations.) The predictions from the 2D model closely follow the measured temperature histories in all three locations. The 1D model shows surprisingly good correlation to the measured temperature at the upper and middle locations, but significantly over predicts temperatures at the lower location.

Temperatures on the inner, unheated surface of the panel for Test 8 are shown in Figure 21. The solid lines represent temperatures measured using the thermocouples with locations shown in Figure 11. The temperatures from the sensors in the heat flux gages are not shown because they gave readings inconsistent with the surrounding thermocouples. Also, results for TC 9 were not available for most tests. The black line is a simple average of the thermocouples shown in the figure. The lines with the dash-dot pattern represent predicted temperatures from the two-dimensional finite element model.

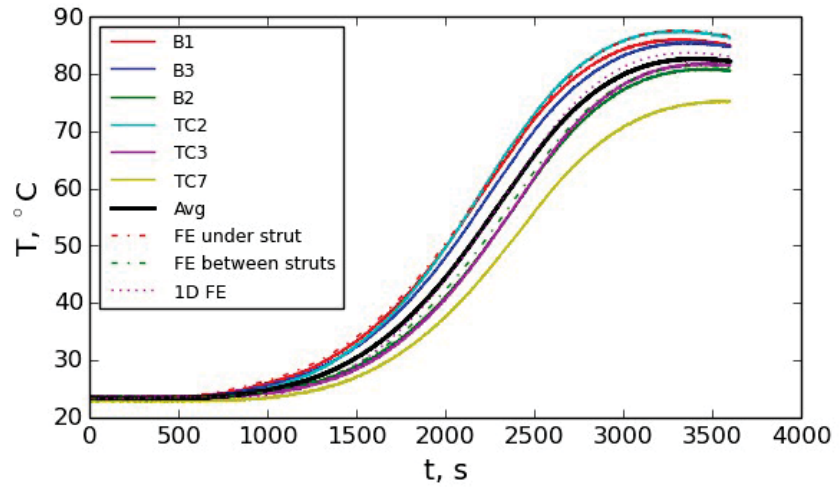


Figure 21: Inner face sheet temperatures for Test 8

The red line is the temperature on the inner face sheet on the extreme left (under the strut) of the 2D model shown in Figure 15, and the green line is on the extreme right of the inner face sheet on the model (between struts). These predictions nearly bound the thermocouple readings near the center of the panel. The temperatures for TC7 are lower, but it is located nearer to the edge of the panel. Predicted temperatures for the one-dimensional model, represented by the dotted line, are between the extremes of the 2D model and agree closely with the average measured temperature history.

Temperatures for the aluminum heat sink, illustrated in Figures 3 and 6, are shown in Figure 22. The solid lines represent temperature readings from two different thermocouples embedded in the heat sink that are nearly identical. The band of oscillations represents the random noise in the thermocouple readings. The dashed lines represent the predicted heat sink temperatures for the 1D and 2D finite element models. The two models agree with each other almost exactly and closely follow the measured temperatures. Notice that the measured temperature rise is only about 3°C.

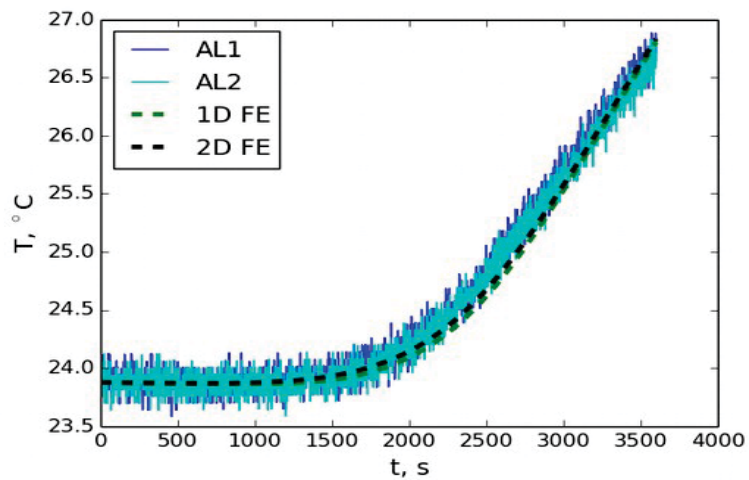


Figure 22: Aluminum heat sink temperatures for Test 8

The average measured temperature for the inner face sheet, illustrated by the black line in Figure 21, is a good indicator of the panel's thermal response to the applied heating (Figure 18) in the ambient gas

composition and pressure for each test. Figure 23 shows the average measured temperature for the inner face sheet for each of the 13 successful tests listed in Table 1. The numbers in the legend of Figure 23 refer to the test number listed in Table 1. The lines are colored according to the applied heating. Red lines represent the BP1 heating profile shown in Figure 13. Black, blue, and green lines represent modified BP3 profiles limited to 540°C, 650°C, and 760°C, respectively. Solid lines represent tests with fixed, low, ambient pressures of either 0.001 or 1 torr. Other line styles represent tests with pressure histories shown in Figure 14. Initial temperatures were not controlled and fluctuated with ambient laboratory temperature and time between tests. The lines illustrate the expected tendency of the maximum inner face sheet temperatures to increase as the heating on the outer face sheet is increased.

The effect of the ambient gas pressure on the maximum inner face sheet temperatures is also apparent in Figure 23. The tests with a fixed ambient pressure of 0.001 torr (solid black, blue, and green lines) result in much lower inner face sheet temperatures than tests with the same heating, but pressure variations simulating atmospheric entry. Test 16, with a fixed pressure of 1 torr, also resulted in lower inner face sheet temperatures than Tests 14 and 15, with variable ambient pressure. Test 5 (blue dotted line) had the same heating and pressure profile as Tests 7 and 8, but was performed in argon rather than nitrogen. The lower thermal conductivity of argon kept the inner face sheet significantly cooler. Comparison of test results and analysis for Test 5 in argon resulted in very similar agreement to that for Test 8, illustrated in Figures 18-20.

For Tests 1, 9, and 10, which were performed with an ambient pressure of 0.001 torr (negligible gas conduction), the predictions from the finite element models did not correlate with the measured temperatures as well as the results shown in Figures 18-20. However, the results for these three tests showed consistent and similar trends with each other. The results for Test 9 are shown in the next three figures because they are typical of these three tests and can be directly compared with the results for Test 8 in Figures 18-20 (same heating with different pressure history.)

The strut temperatures for Test 9 are shown in Figure 24. The solid lines represent measured temperatures on a titanium strut at three different locations

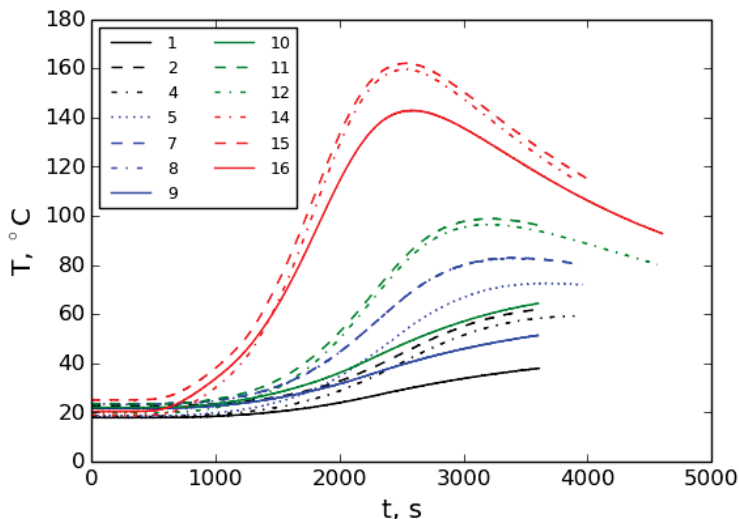


Figure 23: Average inner face sheet temperature for all tests

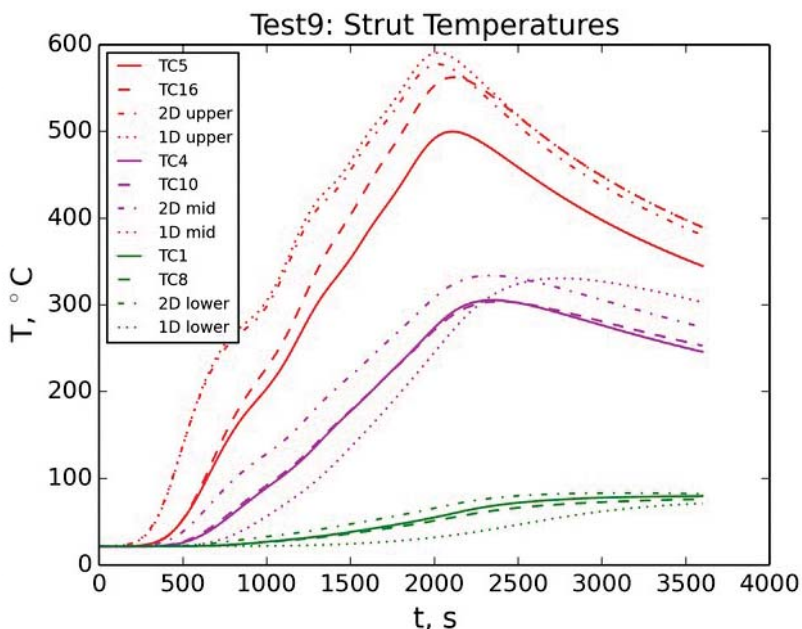


Figure 24: Strut temperatures for Test 9

through the thickness of the panel. Dashed lines represent temperatures at corresponding locations on a nominally identical strut. Thermocouple locations are shown in Figure 10. The dotted lines represent temperature predictions from the 1-D finite element model at the same through-thickness location as the thermocouples. The dot-dash lines represent the temperatures predicted at the same through-thickness locations along the left edge of the 2-D finite element model depicted in Figure 15. Compared to the results for Test 8 (Figure 19), the predictions do not match the measured temperatures as closely. For the location closest to the heated surface, the two models predict that the temperatures rise more quickly and reach a higher temperature than measured. At the mid-thickness location, the 2-D model again predicts the temperature to rise more quickly and reach a higher temperature than the measured values. The response predicted using the 1-D model lags the measured temperatures, but also predicts a higher than measured peak temperature. At the location nearest the unheated surface of the panel, the 2-D model again slightly over predicts the measured temperature. The 1-D model results lag and under predict the measured temperatures.

The insulation temperatures for Test 9 are shown in Figure 25. The solid lines represent the temperatures measured at the thermocouple locations shown in Figure 12. The dotted lines represent temperatures predicted using the 1-D model and the dot-dash lines represent the temperatures predicted along the right edge of the 2-D model illustrated in Figure 15. The 1-D model predicts that the insulation heats up more quickly and to higher temperatures than measured. The 2-D model slightly over predicts the temperatures measured nearest the heated surface, but lags and under predicts the temperatures at the other two locations. The predicted and measured temperatures for Test 9 at 0.001 torr do not match nearly as well as for Test 8 following a simulated entry pressure history (Figure 20.)

Inner face sheet temperatures for Test 9 are shown in Figure 26. The temperatures are significantly lower than those measured in Test 8 and were still increasing when the test was terminated. The solid lines represent temperatures measured using thermocouples at locations

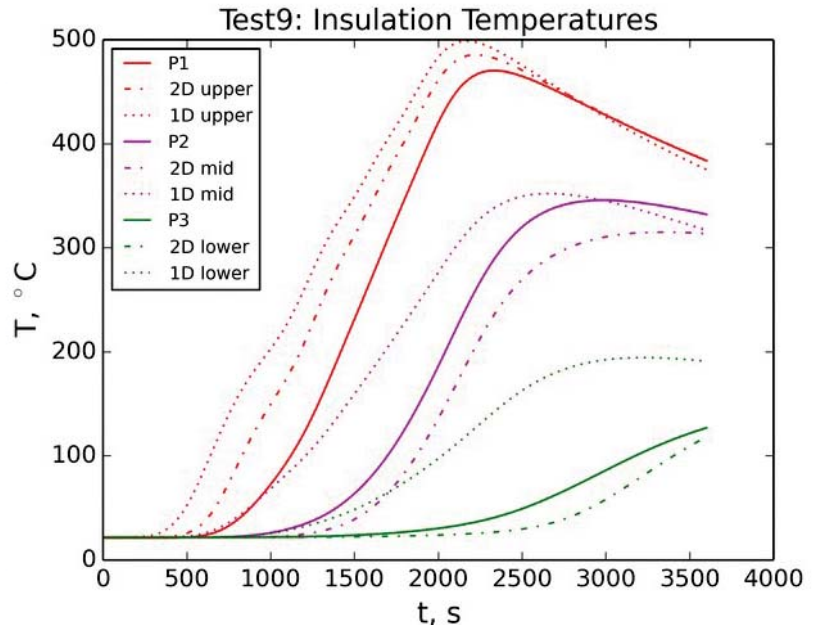


Figure 25: Insulation temperatures for Test 9

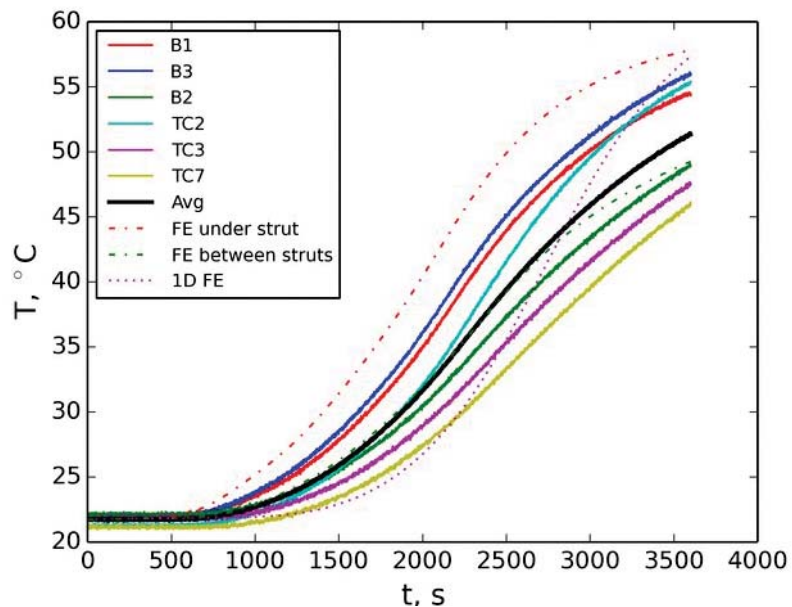


Figure 26: Inner face sheet temperatures for Test 9

shown in Figure 11. The black line is the average of the thermocouple readings shown. The temperature history predicted using the 1-D model initially lags and then significantly overshoots the average measured temperature. The two dot-dash lines represent predictions for the left (red) and right (green) bottom corners of the 2-D model in Figure 15. Although the temperature histories predicted using the 2-D model have a similar shape to measurements, they appear to slightly over predict the measured temperatures. The lowest temperature predicted by the 2-D model is barely under the average measured temperature.

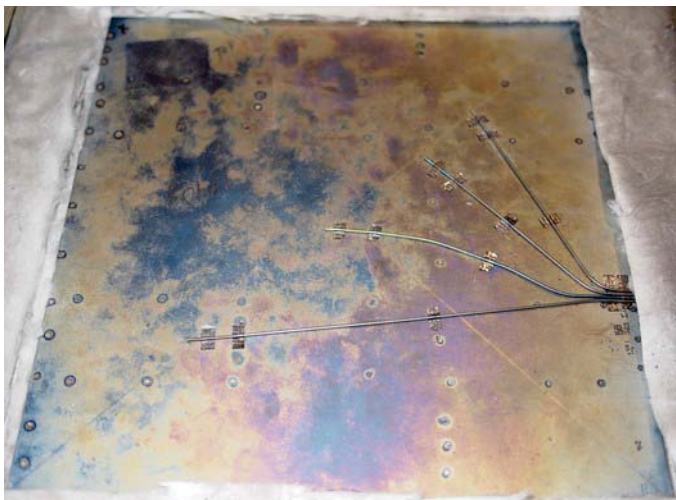


Figure 27: Panel heated surface after Test 12



Figure 28: Panel heated surface after Test 16

After the initially planned tests (through Test 12) were successfully completed and the panel appeared to be in excellent condition (as shown in Figure 27), it was decided to test the panel for the BP1 heating profile shown in Figure 13 (well above any likely reuse temperature for titanium) to see what would happen. Results from Test 14 showed similar trends to previous tests with a simulated entry pressure profile. Test 15 duplicated the heating and pressure profiles of Test 14 with very similar results. Test 16 repeated the BP1 heating profile with a fixed pressure of 1 torr. After these three severe heating cycles, the panel was removed from the testing apparatus for inspection. As shown in Figure 28 the heated surface of the panel warped significantly and blackened. However, the panel remained intact and continued to insulate the inner surface from the applied heating for all of the last three severe thermal cycles.

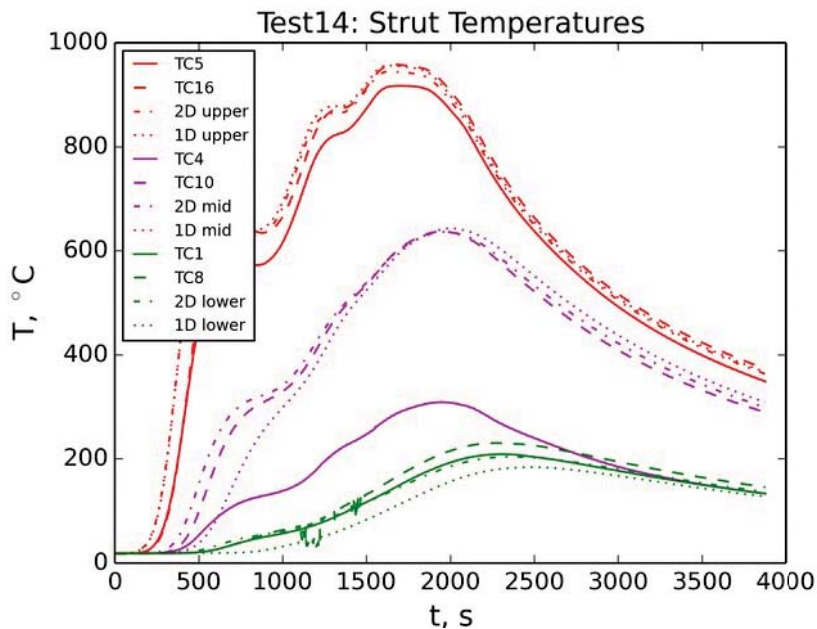


Figure 29: Strut temperatures for Test 14

The strut temperatures for Test 14 are shown in Figure 29. Thermocouple 4 appears to have developed a short and is reading much too low. Thermocouple 8 appears to have shorted intermittently between 1000 and 1500 seconds, but otherwise tracks thermocouple 1. The 2-D finite element predictions follow the measured temperatures fairly closely. The 1-D finite element predictions lag the measured temperatures at the middle and lower locations on the strut.

Remarkably, for this severe heating condition, the correlation between test and analysis is comparable to that for Test 8, shown in Figure 19. Results for Test 15 were nearly identical to those for Test 14.

The insulation temperatures for Test 14 are shown in Figure 30. Both the 1-D and 2-D finite analysis models closely predict the measured temperatures at the upper thermocouple location. Both finite element models under predict the peak measured temperatures at the middle thermocouple location. The 2-D model predictions closely follow the measured temperatures at the lower thermocouple location, but the 1-D model predictions over predict the measured temperatures. Similar trends are seen for Test 8 in Figure 20, although the discrepancy between measurements and predictions are greater for the middle thermocouple location in Test 14. Again, the results for Test 15 are nearly identical to those for Test 14.

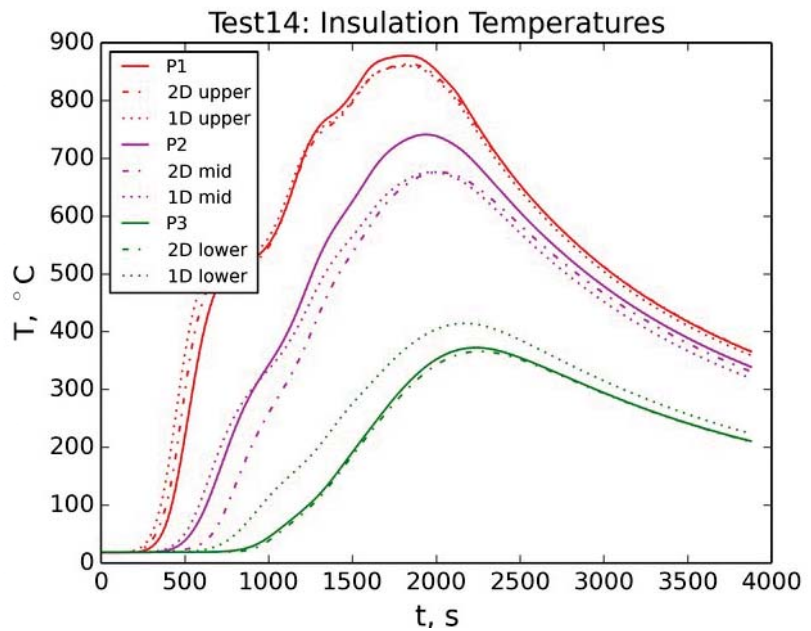


Figure 30: Insulation temperatures for Test 14

The inner face sheet temperatures for Test 14 are shown in Figure 31. Up to about 1000 seconds, the predictions from the 2-D model bracket the readings of the thermocouples near the center of the panel (excluding TC7 which is nearer the panel edge.) After 1000 seconds, the measured temperatures rose more rapidly than predicted and reached peak temperatures 15 to 20°C higher than predicted. This response is different than that for Test 8 (Figure 21) in which the 2-D predicted temperatures bracketed almost perfectly the readings from these same thermocouples. It is difficult to say with certainty why predicted inner face sheet temperatures for Test 14 did not match measurements as well as for Test 8. One possibility is that the temperature dependent material properties are not as accurate at the higher temperatures in Test 14 or that there have been some temperature related changes in the titanium properties. However, the relatively good correlation between test and analysis for the struts and insulation shown in Figures 29 and 30 make this possibility seem unlikely. Another possibility is that panel deformations evident in Figure 28 may have resulted in gaps in the insulation at the panel boundaries or adjacent to some of the titanium struts. Such gaps would result in enhanced heat transfer to the inner face sheet and

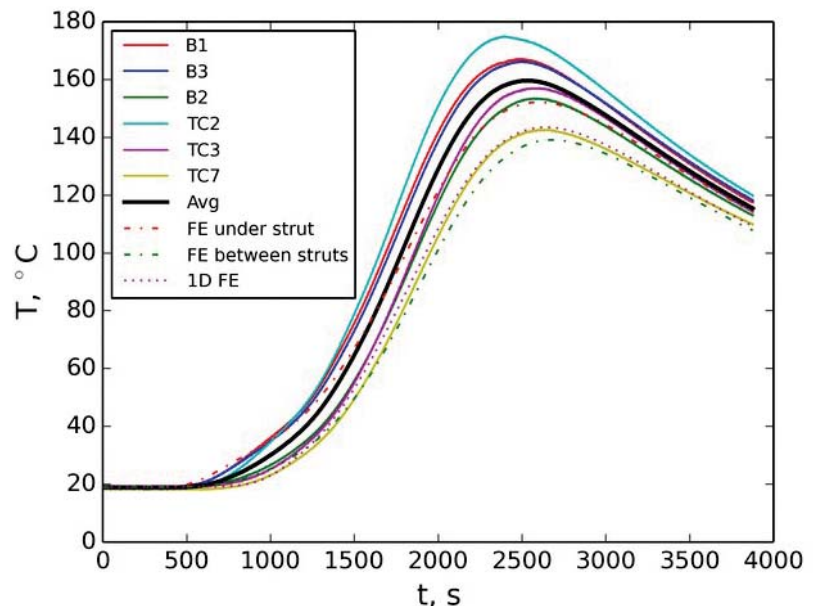


Figure 31: Inner face sheet temperatures for Test 14

would not necessarily be detected by the limited instrumentation through the thickness of the panel. In any case, the panel is well behaved for such a severe heating condition.

The response of the panel for Test 16 was similar to Tests 14 and 15. The inner face sheet temperatures were a bit lower because of the fixed pressure of 1 torr, but correlation between test and analysis was similar that for Test 14, shown in Figures 29-31.

One of the concerns for a relatively complicated thermal-structural test such as this is the repeatability of the results. The test series was structured to provided a number of tests with nominally identical parameters to assess repeatability. Tests 2 and 4, 7 and 9, 11 and 12, as well as 14 and 15 were each repeated tests with the same nominal conditions. One important parameter, the initial temperature distribution was not controlled. The initial temperatures depended on ambient conditions in the laboratory and the time between tests. One way to assess the repeatability of the tests is to look at the difference between the average inner face sheet temperatures for nominally identical tests, as shown in Figure 32. For Tests 7 and 8, the initial average inner face sheet temperature difference is about 0.25°C and remains nearly the same throughout the tests. This result

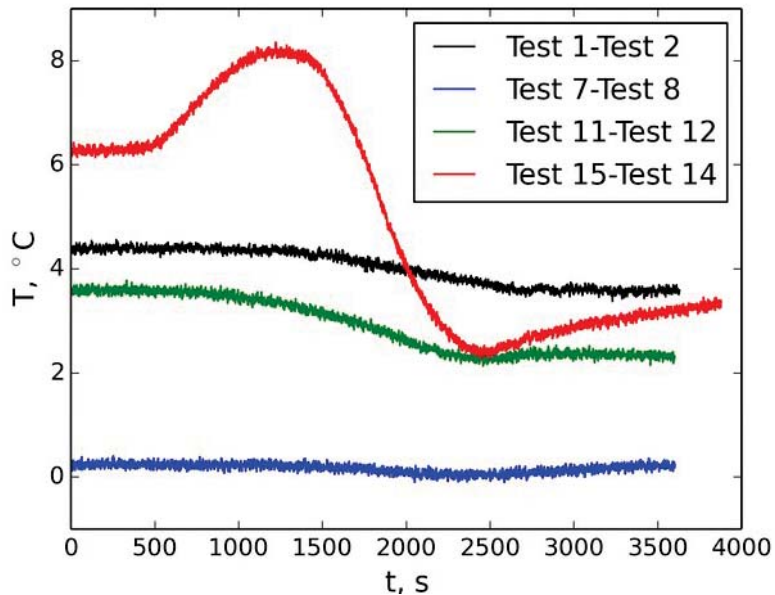


Figure 32: Average inner face sheet temperature difference

demonstrates excellent repeatability. For Tests 1 and 2, and 11 and 12, the initial temperature differences are 4.4°C and 3.6°C, respectively. For both pairs of tests, the temperature differences decrease throughout the tests. Therefore, for these three pairs of tests, any differences appear to be primarily due to variations in the initial temperatures. Variations in other parameters such as heating and pressure profiles appear to be insignificant. Tests 14 and 15 have the largest difference in initial temperature, 6.3°C. The average inner face sheet temperature increases to a maximum of 8.2°C and then decreases below the initial temperature for the latter half of the test. Again, the difference in initial temperatures appears to be the largest factor for the discrepancy between the tests. However, there is an increase above the initial temperature difference that is not understood. Overall, the tests demonstrated excellent repeatability when the initial temperature differences are considered.

Summary

A proposed configuration was devised for the core of a structural sandwich panel that also functions as a thermal insulator. The motivation for this effort is to develop a structural skin for a hypersonic aerospace vehicle that also acts as a thermal protection system. Although the proposed configuration could be fabricated from any of a number of high temperature materials, prototype panels were fabricated from available titanium material. The prototype panels were originally intended as a simple manufacturing demonstration and, consequently, were not sized for any particular set of thermal and structural loads.

Later, it was decided to test one of the panels filled with fibrous insulation under simulated earth entry heating conditions. The purpose of the tests was to measure the thermal response of the panel and compare the measured results to predictions. The panel was heated using a quartz lamp array in a vacuum chamber with carefully controlled boundary conditions. The sides of the panel were well insulated and the unheated side of the panel faced an air gap and an aluminum heat sink with a high emissivity coating. The panel was tested in both argon and nitrogen at very low ambient pressures and with simulated entry pressure histories. Temperatures were measured by numerous type K thermocouples attached to the panel face sheets and embedded through the thickness of the panel. Most of the 13 tests limited the maximum temperature to plausible reusable temperature limits for titanium. However, the last three tests heated the panel to above 1000°C, well above the reusable temperature for titanium. Test results showed that the desired surface temperature was accurately imposed by quartz lamps and that the desired ambient pressure histories were accurately imposed. Excellent repeatability was demonstrated for several different loading conditions.

One- and two-dimensional finite element models of the panel were developed using a program written in the Python programming language. A previously developed model for effective thermal conductivity of the Saffil® insulation as a function of temperature and pressure was incorporated into the finite element models. The geometry of the titanium core was carefully measured and scaled into the simplified 1-D and 2-D finite element models. All material was accurately accounted for and not arbitrarily scaled.

For the simulated entry pressure histories, both the 1-D and 2-D finite element models predicted the inner face sheet temperatures very well. The 1-D model predicted the average of the thermocouples near the center of the panel and the 2-D model bracketed those same thermocouple readings. For the tests with a constant pressure of 0.001 torr, the correlation between test and analysis was not as good. The 1-D model tended to lag the measured response and then overshoot the average inner face sheet temperature. The 2-D model tended to predict the trend correctly, but somewhat over predict the amplitude of the measured inner face sheet temperatures. For the last three hotter tests, both the 1-D and 2-D models under predicted the measured inner face sheet temperatures.

This work is clearly just a first step in assessing the proposed core configuration for a thermally insulating structural panel. Further work needs to be done to size a panel for a realistic set of thermal and mechanical loads and compare it to competing configurations sized for the same loads. If there is a compelling advantage to this configuration, then panels could be fabricated and tested to verify the predicted performance.

Although additional work is needed, results have demonstrated that a relatively complex geometry panel can be accurately represented using models with simplified geometry. Such simplified models could be readily incorporated into a thermal-structural optimization to identify promising panel configurations.

References

1. Bapanapalli, S. K., Martinez, O. M., Gogu, C., Sankar, B. V., Haftka, R. T., and Blosser, M. L., "Analysis and design of corrugated core sandwich panels for thermal protection systems of space vehicles," AIAA paper 2006-1942, 2006.
2. Martinez, O., Bapanapalli, S. K., Sankar, B. V., Haftka, R. T., and Blosser, M. L., "Micromechanical analysis of composite truss-core sandwich panels for integral thermal protection systems," AIAA paper 2006-1876, 2006.
3. Gogu, C., Bapanapalli, S. K., Haftka, R. T., Sankar, B. V., "Comparison of materials for integrated thermal protection systems for spacecraft reentry," Journal of Spacecraft And Rockets, 46(3), 2009: 501-513.
4. Brewer, Amy R., "Edgewise compression testing of SITPS-0 (Structurally Integrated Thermal Protection System)," NASA/CR-2011-217161, July 2011.

5. Daryabeigi, Kamran, George R. Cunningham, and Jeffrey R. Knutson. "Combined heat transfer in high-porosity high-temperature fibrous insulation: Theory and experimental validation." *Journal of Thermophysics and Heat Transfer* 25(4), 2011: 536-546.
6. Daryabeigi, Kamran, Jeffrey R. Knutson, and George R. Cunningham. "Heat transfer measurement and modeling in rigid high-temperature reusable surface insulation tiles." *AIAA Paper* 2011-345, 2011.
7. Blosser, Max. "Boundary conditions for aerospace thermal-structural tests." *PROGRESS IN ASTRONAUTICS AND AERONAUTICS* 168, 1995: 119-144.
8. Daryabeigi, Kamran, Jeffrey R. Knutson, and Joseph G. Sikora. "Thermal vacuum facility for testing thermal protection systems." *NASA TM-2002-211734*, 2002.
9. Ko, William L., Robert D. Quinn, and Leslie Gong. "Finite-element reentry heat-transfer analysis of Space Shuttle Orbiter." *NASA TP* 2657, 1986.
10. Gong, Leslie, Robert D. Quinn, and William L. Ko. "Reentry heating analysis of space shuttle with comparison of flight data." *Computational Aspects of Heat Transfer in Structures*. Vol. 1. 1982.
11. Myers, David E., Carl J. Martin, and Max L. Blosser. "Parametric weight comparison of current and proposed thermal protection system (TPS) concepts." *NASA TM-2000-210289*, June 2000.
12. Poteet, Carl C., Hasan Abu-Khajeel, and Sun-Yuen Hsu. "Preliminary thermal-mechanical sizing of a metallic thermal protection system." *Journal of Spacecraft and Rockets* 41(2), 2004: 173-182.
13. Blosser, Max L. "Fundamental modeling and thermal performance issues for metallic thermal protection system concept." *Journal of Spacecraft and Rockets* 41(2), 2004: 195-206.
14. Turner, Travis L., and Robert L. Ash. "Numerical and experimental analyses of the radiant heat flux produced by quartz heating systems." *NASA TP* 3387, 1994.
15. Logg, Anders, Garth N. Wells, and Johan Hake. *DOLFIN: A C++/Python finite element library*. Springer Berlin Heidelberg, 2012.

REPORT DOCUMENTATION PAGE

*Form Approved
OMB No. 0704-0188*

The public reporting burden for this collection of information is estimated to average 1 hour per response, including the time for reviewing instructions, searching existing data sources, gathering and maintaining the data needed, and completing and reviewing the collection of information. Send comments regarding this burden estimate or any other aspect of this collection of information, including suggestions for reducing this burden, to Department of Defense, Washington Headquarters Services, Directorate for Information Operations and Reports (0704-0188), 1215 Jefferson Davis Highway, Suite 1204, Arlington, VA 22202-4302. Respondents should be aware that notwithstanding any other provision of law, no person shall be subject to any penalty for failing to comply with a collection of information if it does not display a currently valid OMB control number.
PLEASE DO NOT RETURN YOUR FORM TO THE ABOVE ADDRESS.

1. REPORT DATE (DD-MM-YYYY) 01-03 - 2015		2. REPORT TYPE Technical Memorandum		3. DATES COVERED (From - To)	
4. TITLE AND SUBTITLE Transient Thermal Testing and Analysis of a Thermally Insulating Structural Sandwich Panel				5a. CONTRACT NUMBER	
				5b. GRANT NUMBER	
				5c. PROGRAM ELEMENT NUMBER	
6. AUTHOR(S) Blosser, Max L.; Daryabeigi, Kamran; Bird, R. Keith; Knutson, Jeffrey R.				5d. PROJECT NUMBER	
				5e. TASK NUMBER	
				5f. WORK UNIT NUMBER 736466.01.08.07.31	
7. PERFORMING ORGANIZATION NAME(S) AND ADDRESS(ES) NASA Langley Research Center Hampton, VA 23681-2199				8. PERFORMING ORGANIZATION REPORT NUMBER L-20546	
9. SPONSORING/MONITORING AGENCY NAME(S) AND ADDRESS(ES) National Aeronautics and Space Administration Washington, DC 20546-0001				10. SPONSOR/MONITOR'S ACRONYM(S) NASA	
				11. SPONSOR/MONITOR'S REPORT NUMBER(S) NASA-TM-2015-218701	
12. DISTRIBUTION/AVAILABILITY STATEMENT Unclassified - Unlimited Subject Category 34 Availability: NASA STI Program (757) 864-9658					
13. SUPPLEMENTARY NOTES					
14. ABSTRACT A core configuration was devised for a thermally insulating structural sandwich panel. Two titanium prototype panels were constructed to illustrate the proposed sandwich panel geometry. The core of one of the titanium panels was filled with Saffil® alumina fibrous insulation and the panel was tested in a series of transient thermal tests. Finite element analysis was used to predict the thermal response of the panel using one- and two-dimensional models. Excellent agreement was obtained between predicted and measured temperature histories.					
15. SUBJECT TERMS Sandwich panel; Thermal analysis; Thermal protection system; Thermal testing					
16. SECURITY CLASSIFICATION OF:			17. LIMITATION OF ABSTRACT	18. NUMBER OF PAGES	19a. NAME OF RESPONSIBLE PERSON
a. REPORT	b. ABSTRACT	c. THIS PAGE			STI Help Desk (email: help@sti.nasa.gov)
U	U	U	UU	27	19b. TELEPHONE NUMBER (Include area code) (757) 864-9658